Am J Transl Res 2019;11(5):2995-3006
www.ajtr.org /ISSN:1943-8141/AJTR0091436

Original Article

Tanshinone IIA induces apoptosis and autophagy in acute monocytic leukemia via downregulation of PI3K/Akt pathway

Yanping Zhang[1], Yan Geng[1], Juntao He[1], Dong Wu[2], Tong Zhang[1], Li Xue[1], Lei Zhang[1], Aili He[2]

Departments of [1]Laboratory, [2]Hematology, The Second Affiliated Hospital of Xi'an Jiaotong University, Xi'an 710004, P. R. China

Received January 17, 2019; Accepted April 29, 2019; Epub May 15, 2019; Published May 30, 2019

Abstract: Acute myeloid leukemia (AML) is characterized by unrestrained proliferation of myeloid cells. In has been shown that tanshinone IIA (Tan IIA), exhibited anti-tumor activities on different types of cancers. However, the underlying mechanisms by which Tan IIA regulates apoptosis and autophagy in AML remain unclear. Thus, this study aimed to investigate the effects of Tan IIA on AML *in vitro* and *in vivo*. CCK-8 assay, EdU staining, flow cytometry, MDC staining, immunofluorescence, transwell migration and invasion assay were used to detect cell proliferation, apoptosis, autophagy, migration and invasion, respectively. In addition, western blotting was used to examine the protein levels of Bax, Bcl-2, active caspase-3, Beclin-1, Atg-5, p-mTOR and p-Akt in cells. Moreover, animal studies were performed to evaluate anti-tumor effect of Tan IIA on AML *in vivo*. The results revealed that Tan IIA significantly suppressed the growth of U937 cells *in vitro* and *in vivo*. Meanwhile, Tan IIA induced apoptosis in U937 cells via up-regulating the levels of active caspase-3 and Bax, and down-regulating Bcl-2 *in vitro* and *in vivo*. In addition, Tan IIA inhibited the capacity of migration and invasion in U937 cells. Moreover, Tan IIA induced autophagy in U937 cells via upregulation of the expression of LC3 II, Atg5 and Beclin 1, which was further confirmed by MDC staining and immunofluorescence assays. For the first time, we have shown that autophagy inhibitor 3MA significantly enhanced Tan IIA-induced apoptosis in U937 cells. Furthermore, Tan IIA induced apoptosis and autophagy via downregulation of PI3K/Akt pathway *in vitro* and *in vivo*. Therefore, the accumulating evidences suggested that Tan IIA could be a potential agent for improving the symptoms of AML in the future.

Keywords: Tanshinone IIA, acute monocytic leukemia, apoptosis, autophagy, PI3K/Akt pathway

Introduction

AML is a kind of leukemia, which is characterized by the abnormal accumulation of marrow cells [1, 2]. The 5-year mortality rate of patients is more than 70% [3]. The older patients who diagnosed with acute monocytic leukemia have a pretty poor prognosis due to the therapy-triggered negative effects, their average overall survival is only 5 to 10 months [4]. Although only 10-20% of children patients diagnosed with AML cannot receive chemical therapy properly, reappear occurs in 30-40% of children patients with AML [5-7]. Therefore, more effective therapeutic strategies for treating AML need to be discovered.

Tanshinone IIA (Tan IIA) is one of the vital fat-soluble monomer components, which extracted from Chinese herbal medicine Salvia miltiorrhiza Bge [8, 9]. Tan IIA has been used as an effective monomeric compound to remedy patients with osteosarcoma cancer, parkinson's disease and oral squamous cell carcinoma [10-12]. Several studies showed that Tan IIA exhibited anti-inflammatory and anti-oxidative functions in rats [13, 14]. Previous study also found that Tan IIA could inhibit proliferation, invasion and migration in osteosarcoma MG-63 cells [10]. However, the effects of Tan IIA on the AML remain unclear.

Autophagy and apoptosis are important mechanisms to keep a stabilized cellular environment, which are involved in cell growth, differentiation and other physiological processes [15, 16]. PI3K/Akt signaling pathway is a vital intracellular signal transduction pathway, which plays a

very important role during the development and progression of cancer [17]. Li et al studied that Tan IIA could improve the symptom of myocardial ischemia reperfusion injury through regulating the PI3K/Akt/mTOR signaling pathway [18]. Moreover, Tan IIA could induce autophagy in oral squamous carcinoma cell via suppressing the PI3K/Akt/mTOR pathway [12]. Hence, we investigated the effects of Tan IIA on the proliferation, apoptosis and autophagy of AML *in vitro* and *in vivo*.

Materials and methods

Cell culture

The human U937 cell line was obtained from American Type Culture Collection (ATCC, Rockville, MD, USA). Cells were cultured in Dulbecco's Modified Eagle's Medium (DMEM, Thermo Fisher Scientific, Waltham, MA, USA) supplemented with 10% heat-inactivated fetal bovine serum (FBS, Thermo Fisher Scientific), penicillin and streptomycin (100 U/ml, Thermo Fisher Scientific) in a humidified incubator with 5% CO_2 at 37°C.

CCK-8 assay of cell viability

Cell viability was assessed with Cell Counting Kit-8 (CCK8, Beyotime, Shanghai, China) according to the manufacturer's protocols. U937 cell lines were seeded into a 96-well plate at a density of 5×10^3 cells/well and incubated at 37°C. Then, cells were incubated with Tan IIA or 3MA. After incubation, 10 μL of CCK-8 reagent was added to each well and then incubated for 2 h. The absorbance was determined at 450 nm using a microplate reader (Bio-Rad, Hercules, CA, USA) using wells without cells as blanks. Tan IIA standard product was purchased from sigma (Sigma, St. Louis, MO, USA, # T4952).

EdU staining

U937 cell lines were seeded into a 24-well plate at a density of 4×10^5 cells/well and incubated at 37°C overnight. Then, the cell were treated with different concentrations of Tan IIA (0, 20 or 40 μM) and incubated for 72 h. Harvested U937 cells (1×10^6 cells) were incubated with 50 μM EdU labeling medium at 37°C for 2 h. EdU detection was performed according to the EdU kit specification (Thermo Fisher Scientific, Waltham, MA, USA) described method.

Colony-forming unit (CFU) assay

Colony-forming unit-U937 were cultured in methylcellulose (1%) supplemented with fetal bovine serum (FBS, 30%), 1% BSA, 0.1 mM β-mercaptoethanol, and Tan IIA (20 or 40 μM). U937 cells (2×10^4 cells/mL) were seeded into a 6-well plate and incubated for 3 days. The colony was considered as a cluster of 50 or more cells. Colonies were scored blindly.

Flow cytometric analysis of cell apoptosis

Annexin V-FITC Apoptosis Detection Kit (Thermo Fisher Scientific, #V13241) was used to evaluate the percentage of apoptosis cells according to the manufacturer's protocols. U937 cell lines were seeded into a 6-well plate and incubated at 37°C overnight. Then, cells were incubated with Tan IIA or 3MA for 72 h. Cultured cells (5×10^5 cell/well) were centrifuged at 1000 g at room temperature for 5 min followed by washing with cold phosphate-buffered saline (PBS) 3 times. Afterwards, pelleted cells were stained with 5 μL Annexin V and 5 μL propidium iodide (PI) in 500 μL apoptosis reaction solution for 15 min at room temperature in the dark following the manufacture's instruction, and analyzed by flow cytometry (Dickinson Franklin Lake, NJ, USA) using a FACScan™ flow cytometry system.

Western blot analysis

Cells were washed with PBS twice and lysed in cell lysis buffer. Cell lysates were clarified by centrifugation at 12,000 *g* for 10 min at 4°C, and the supernatants were mixed with 4 × loading buffer (Thermo Fisher Scientific) and boiled for 5 min. The protein contents in the supernatant were measured by using a Bradford Protein Assay Kit (Beyotime, Shanghai, China). Proteins were separated by electrophoresis with 10% SDS polyacrylamide gel, and then proteins were transferred onto polyvinylidene fluoride membranes (PVDF, Thermo Fisher Scientific, Waltham, MA, USA) in 2 h. The membranes were blocked with 5% skim milk for 1 h at room temperature. After that, membranes were incubated with primary antibodies overnight at 4°C: anti-Bax (Abcam; ab32503) (1:1000), anti-Bcl-2 (Abcam, Cambridge, MA, USA; ab32124) (1:1000), anti-active caspase 3 (Abcam; ab2302) (1:1000), anti-β-actin (Abcam; ab8227) (1:1000), anti-Beclin 1 (Abcam; ab207612) (1:1000), anti-Atg 5 (Abcam; ab228668) (1:1000).

After washing, the PVDF membrane was incubated with secondary antibody anti-rabbit (Abcam; ab7090) (1:5000) for 1 h at room temperature before determined by chemiluminescence. Finally, the PVDF membranes were incubated with ECL reagent (Santa Cruz Biotechnology) to detect the blots.

Transwell migration assay

The cell migration assay was conducted using a 24-well transwell chambers according to the manufacturer's protocols (BD, Franklin Lake, NJ, USA). Briefly, U937 cells (4×10^5 cells/well) were seeded onto the upper chamber (Corning, NY, USA) in 200 μL serum-free medium. The lower wells were added into 500 μL DMEM medium containing with 10% FBS. After 24 h of incubation at 37°C, cells that invaded through the membrane were fixed with 4% paraformaldehyde and then stained with 0.05% crystal violet for 2 h. Finally, invaded cells were counted under a microscope at a magnification of × 200 and the relative number was calculated.

Transwell invasion assay

The cell invasiveness assay was conducted using a 24-well matrigel chambers according to the manufacturer's protocols (BD, Franklin Lake, NJ, USA). Transwell membranes (polycarbonic membrane, diameter 6.5 mm, pore size 8 μm) were coated with matrigel in a total of 50 μL each transwell (matrigel/serum free medium: 1/5). U937 cells (4×10^5 cells/well) were seeded onto the upper chamber (Corning, NY, USA) in 200 μL serum-free medium. The lower wells were added into 500 μL DMEM medium containing with 10% FBS. After 24 h of incubation at 37°C, cells that invaded through the matrigel membrane were fixed with 4% paraformaldehyde and stained with 0.05% crystal violet for 2 h. Finally, invaded cells were counted under a microscope at a magnification of × 200 and the relative number was calculated.

Monodansylcadaverine (MDC) staining

U937 cell lines were seeded into a 6-well plate and incubated at 37°C overnight. Then, cells were incubated with Tan IIA or 3MA for 72 h. Then, cells were stained with 0.05 mM MDC (Sigma Aldrich, St. Louis, MO, USA, #D4008) at 37°C for 30 min. After that, U937 cells were washed with PBS twice to wipe off redundant MDC. Fluorescence of cells were instantly observed and counted with a Hitachi F-2000 fluorescence spectrophotometer (Olympus Corporation, Tokyo, Japan) and counting.

Immunofluorescence

Cultured cells were washed in PBS 3 times, prefixed in 4% paraformaldehyde at room temperature for 15 min, and then fixed in pre-cool methanol (100%) for 10 min at -20°C. Next, cells were incubated with primary antibodies for DAPI (Abcam; ab104139) and LC3 (Abcam; ab48394) overnight at 4°C. Then, cells were incubated with goat anti-rabbit secondary antibody, (Thermo Fisher Scientific, Alexa Fluor 488, #R37116) (1:1000) at 37°C for 1 h. The samples were immediately observed by fluorescence microscope (Olympus CX23 Tokyo, Japan).

Animal study

Male BALB/nude mice (aged 4-6 weeks) were purchased from Shanghai Slac Animal Center (Shanghai, China) and housed within a dedicated SPF facility with alternating 12 h periods of light and darkness, a constant temperature of 18-23°C and 55-65% humidity. Aliquots of U937 cells (1×10^7 cells, in 100 μL of PBS) were injected subcutaneously into the right flank. The tumor growth and body weight of the mice were monitored every day. When the tumors volume reached to 100 mm^3, the nude mice were randomly divided into treatment and vehicle groups (n = 4 mouse/group). The vehicle group received normal saline only. In the treatment groups, mice were intraperitoneal (ip) injection with 30 or 50 mg/kg Tan-IIA, respectively; three times a week for 4 weeks. Mice were weighted weekly. Tumor volume was measured by calipers every week until mice were sacrificed under anesthesia. Inhibition rate of tumor growth (X) was measuring by the weight of the tumor (W) and using the equation $X = (W_{vehicle}-W_{Tan\text{-}IIA})/W_{vehicle}$ All animal experiments were performed in accordance with institutional guidelines, following a protocol approved by the Ethics Committees of the Second Affiliated Hospital of Xi'an Jiaotong University.

TUNEL staining

Deparaffinized tissue sections were stained using an APO-BrdU™ TUNEL Assay Kit (Thermo Fisher Scientific, Waltham, MA, USA), according to the manufacturer's instructions.

Statistical analysis

Each group were executed at least three independent experiments and all data were expressed as the mean ± SD. Statistical analysis of data was performed using SPSS version 13.0 (SPSS Inc, Chicago, IL). The results of the transwell migration and invasion assays were analyzed by Student's t-test. The differences in the cell proliferation, cell autophagy and cell apoptosis assays were analyzed by one-way analysis of variance (ANOVA) followed by Dunnett's test. $P < 0.05$ or $P < 0.01$ was considered to indicate a statistically significant difference (*$P < 0.05$, **$P < 0.01$).

Results

Tan IIA inhibited proliferation and colony formation in U937 cells

The chemical structure of Tan IIA is presented in **Figure 1A**. CCK-8 assays were used to detect the viability of U937 cells after treatment with various concentrations of Tan IIA for 24, 48 and 72 h. As presented in **Figure 1B**, Tan IIA inhibited U937 cell growth in a dose- and time-dependent manners. Since, Tan IIA (20 and 40 μM) induced about 50% growth inhibition, Tan IIA at 20 and 40 μM doses were utilized in the following *in vitro* experiments. In addition, the results of EdU fluorescence assay indicated that the EdU positive cells were significantly decreased by Tan IIA treatment, compared with the control group (**Figure 1C** and **1D**). Furthermore, colony formation assay indicated that Tan IIA markedly inhibited proliferation in U937 cells (**Figure 1E** and **1F**). These results suggested that Tan IIA could suppress proliferation and colony formation in U937 cells.

Tan IIA induced apoptosis in U937 cells

In order to investigate the effect of Tan IIA on apoptosis of U937 cells, Annexin V/PI staining was applied. As indicated in **Figure 2A** and **2B**, Tan IIA significantly induced apoptosis in U937 cells, compared with the control group. Next, the levels of apoptosis-related proteins Bax, Bcl-2 and active-caspase 3 were detected by western blotting. The results showed the expressions of Bax and active caspase 3 were markedly increased, while the level of Bcl-2 was significantly decreased in 40 μM Tan IIA-treated group, compared with the control group (**Figure 2C-F**). All these results indicated that Tan IIA could induce apoptosis in U937 cells.

Tan IIA inhibited the capacity of migration and invasion in U937 cells

Next, the transwell assays were used to investigate the effects of Tan IIA on the migration and invasion abilities of U937 cells [19]. The results revealed that 40 μM Tan IIA significantly decreased the capacity of migration and invasion in U937 cells, compared with the control group (**Figure 3A-D**). These data suggested that Tan IIA could inhibit the capacity of migration and invasion in U937 cells.

Inhibition of autophagy enhanced Tan IIA-induced apoptosis in U937 cells

In order to assess the role of Tan IIA on the autophagy of U937 cells, MDC assay and immunofluorescence assay were performed. The MDC staining data indicated that the autophagic vacuoles and autophagosome was dramatically increased in the U937 cells by Tan IIA treatment, compare with the control group (**Figure 4A** and **4B**). Additionally, immunofluorescence data indicated that Tan IIA increased the level of LC3-II, which positively related with autophagosome formation (**Figure 4C**). Western blotting was then utilized to detect the expressions of autophagy-related proteins Beclin 1 and ATG 5 in the U937 cells. As revealed in **Figure 4D-F**, compare with the control group, Tan IIA dramatically increased the levels of Beclin 1 and ATG 5 in U937 cells. These data revealed that Tan IIA could induce autophagy in U937 cells.

In addition, autophagy inhibitor 3MA was used to further testify the effect of Tan IIA on U937 cells. Compared with the Tan IIA-treated group, the number of proliferative cells were significantly decreased, while the apoptotic cells were markedly increased in the presence of 3MA, respectively (**Figure 4G-I**). As expected, the level of active caspase 3 in cells were further increased by 3MA, compared with Tan IIA alone (**Figure 4J** and **4K**). All these results suggested that inhibition of autophagy could enhance Tan IIA-induced apoptosis in U937 cells.

Tan IIA induced autophagy in U937 cells via downregulation of PI3K/Akt pathway

Previous studies showed that PI3K/Akt pathway plays an important role in regulation of cell autophagy [20, 21]. To further explore the me-

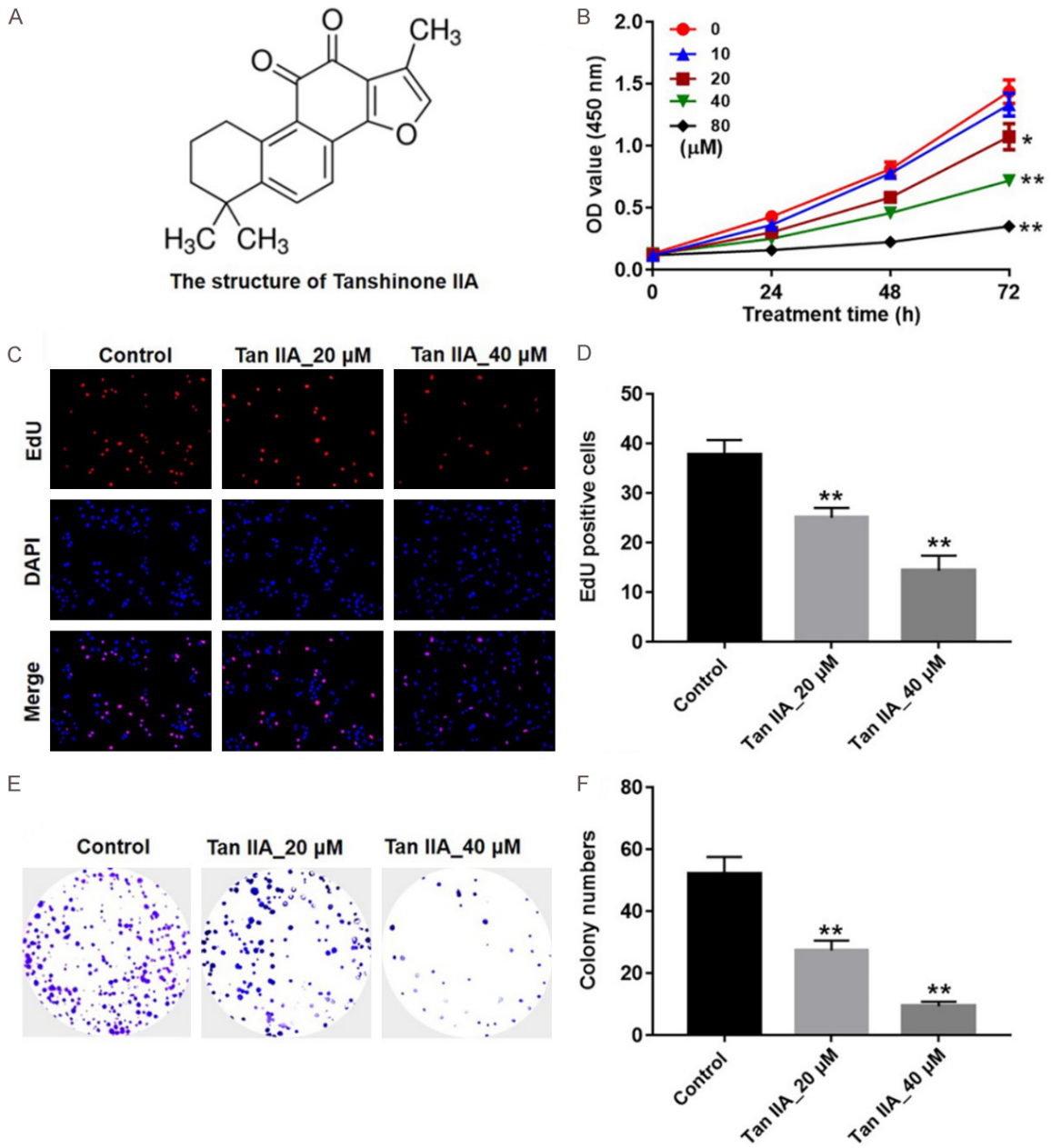

Figure 1. Tan IIA inhibited U937 cell proliferation. A. The chemical structure of Tan IIA. B. Cell viability was determined using CCK-8 assay in U937 cells treated with emodin (0, 10, 20, 40 or 80 μM) for 24, 48 and 72 h. C, D. U937 cells were treated with Tan IIA (20 or 40 μM) for 72 h. Relative fluorescence expressions were quantified by EdU and DAPI staining. E, F. U937 cells were underwent a colony formation assay for 3 days, and surviving colonies were counted. (*P < 0.05, **P < 0.01 vs. control).

chanism by which Tan IIA regulated autophagy on U937 cells, western blotting was utilized to detect the expressions of p-Akt and p-mTOR. As shown in **Figure 5A-C**, Tan IIA markedly down-regulated the levels of p-mTOR and p-Akt in U937 cells compared with the control group (**Figure 5A-C**). These data suggested that Tan IIA induced autophagy in U937 cells via down-regulation of PI3K/Akt pathway.

Tan IIA inhibited tumor growth via induction of apoptosis in vivo

In order to evaluate the anti-tumor effect of Tan IIA *in vivo*, U937 tumor bearing xenograft was applied. As shown in **Figure 6A-C**, both 30 and 50 mg/kg Tan IIA significantly inhibited tumor growth and tumor weight, compared with vehicle group. In addition, the tumor growth inhibi-

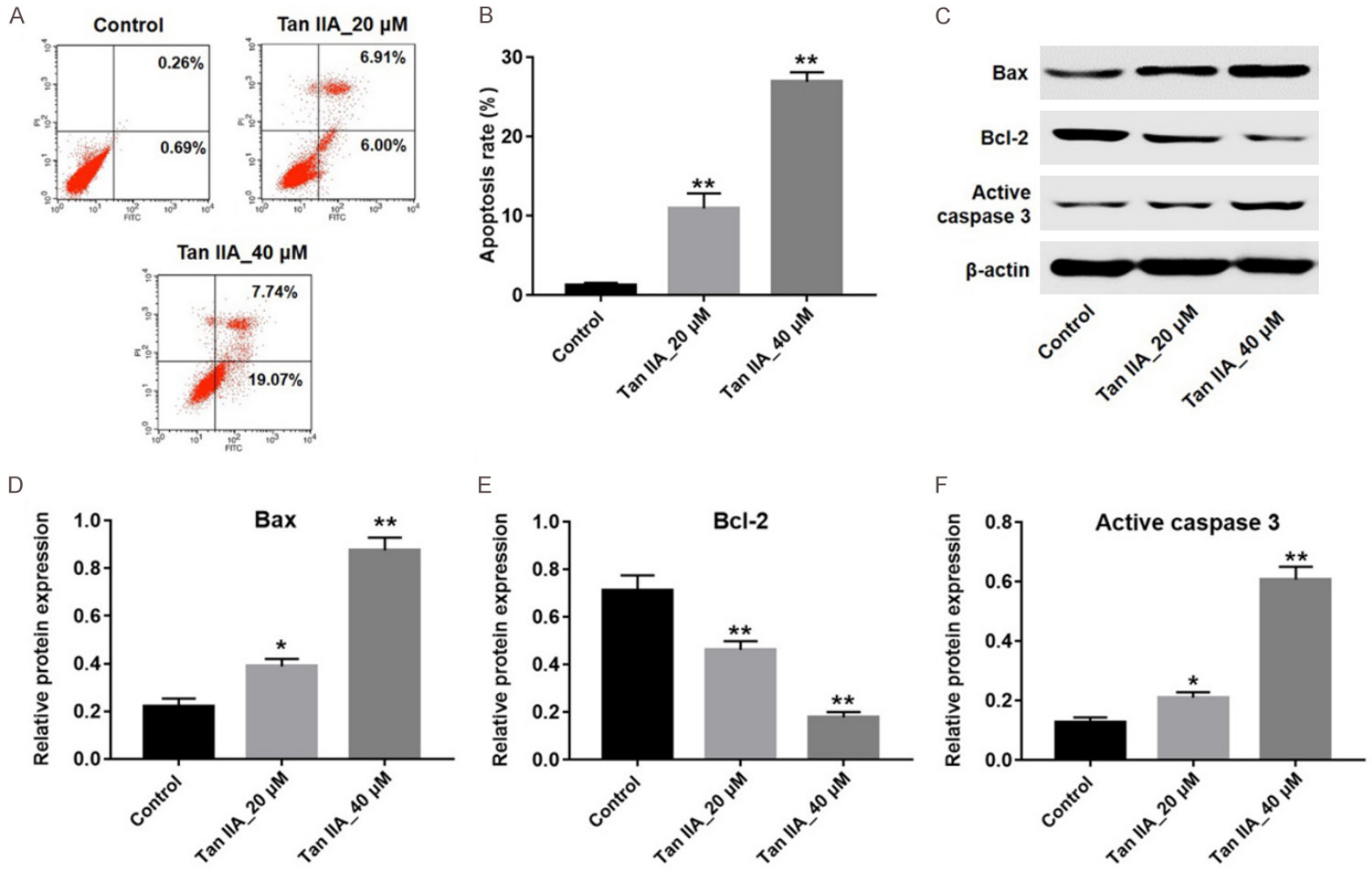

Figure 2. Tan IIA induced apoptosis in U937 cells. U937 cells were exposed to 20 or 40 μM Tan IIA for 72 h. A. Apoptotic cells were detected with Annexin V and PI double staining. B. Apoptosis cell rates were calculated. C. Expressions of Bax, Bcl-2 and active caspase-3 in U937 cells were analyzed by western blotting. D. The expression of Bax was quantified by normalizing to β-actin. E. The expression of Bcl-2 was quantified by normalizing to β-actin. F. The expression of active caspase-3 was quantified by normalizing to β-actin. (*P < 0.05, **P < 0.01 vs. control).

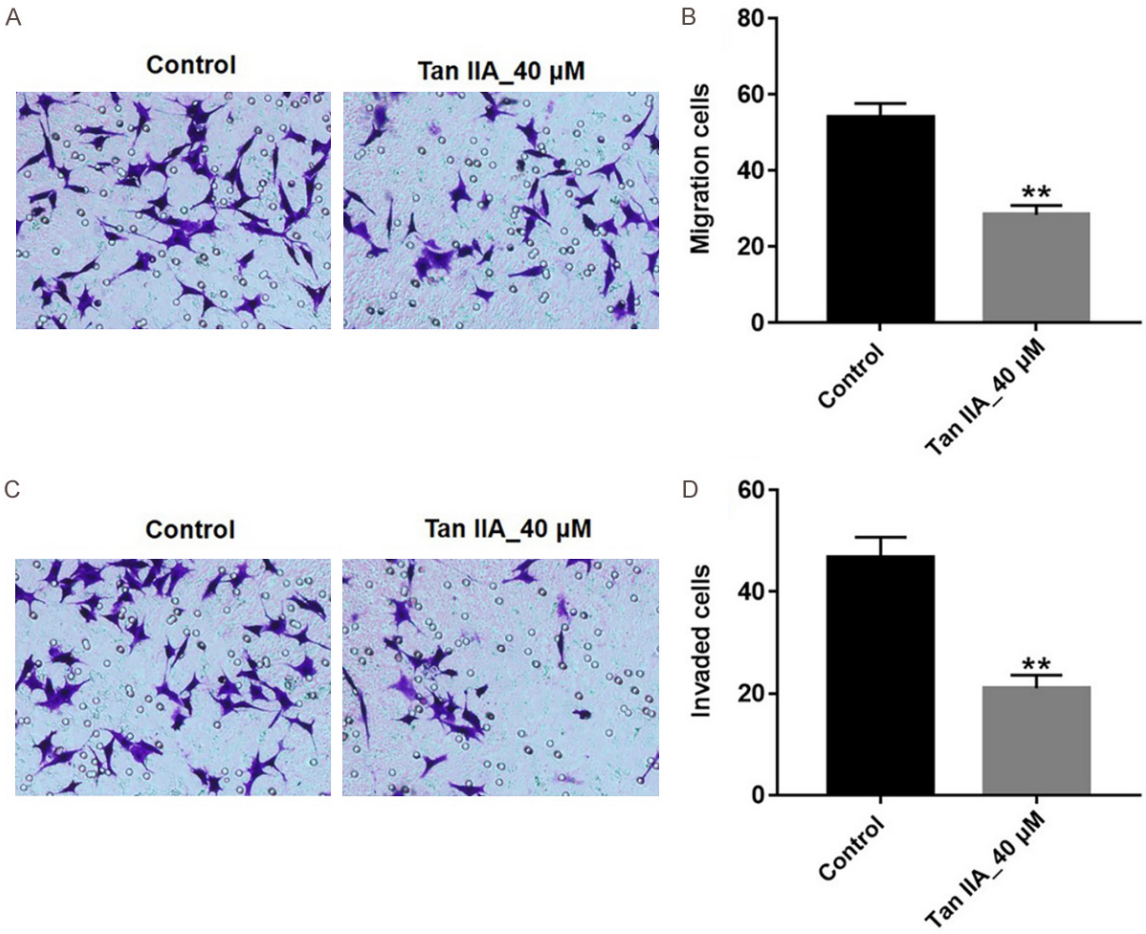

Figure 3. Tan IIA inhibited the capacity of migration and invasion in U937 cells. U937 cells were exposed to 40 μM Tan IIA for 24 h. A, B. Cell migration ability was detected using transwell migration assay, × 200 magnification. C, D. Cell invasion ability was detected using transwell invasion assay, × 200 magnification. **P < 0.01 vs. control.

tion rate in 30 and 50 mg/kg Tan IIA treatment group were approximately 40% and 70%, respectively (**Figure 6D**). Moreover, the results of TUNEL indicated that either 30 or 50 mg/kg of Tan IIA significantly increased cell apoptosis in tumor tissues (**Figure 6E** and **6F**).

To clarify the molecular mechanisms underlying the anti-tumor effect of Tan IIA *in vivo*, expressions of apoptosis- and autophagy- related proteins were detected by western blot. As shown in **Figure 6G-J**, the levels of p-mTOR and p-Akt were markedly decreased, whereas the level of Beclin 1 was notably increased in Tan IIA-treated groups. All these results verified that Tan IIA inhibited U937 cell growth via downregulation of p-mTOR and p-Akt and upregulation Beclin 1 *in vitro* and *in vivo*.

Discussion

In this study, we revealed that Tan IIA induced apoptosis and autophagy on U937 cells *in vitro* and *in vivo*. This finding highlights that inhibition of autophagy increased Tan IIA-induced apoptosis in U937 cells, indicating that autophagy may play a protective role in U937 cells. To the best of our knowledge, this is the first report of the effects of Tan IIA on U937 cells *in vitro* and *in vivo*.

Previous studies have shown that Tan IIA could inhibit cell proliferation in gastric cancer and breast cancer [22, 23]. The results of the present study revealed that Tan IIA inhibited proliferation in a dose and time-dependent manners in U937 cells. In addition, Tan IIA significantly reduced the volume and the weight of the cervi-

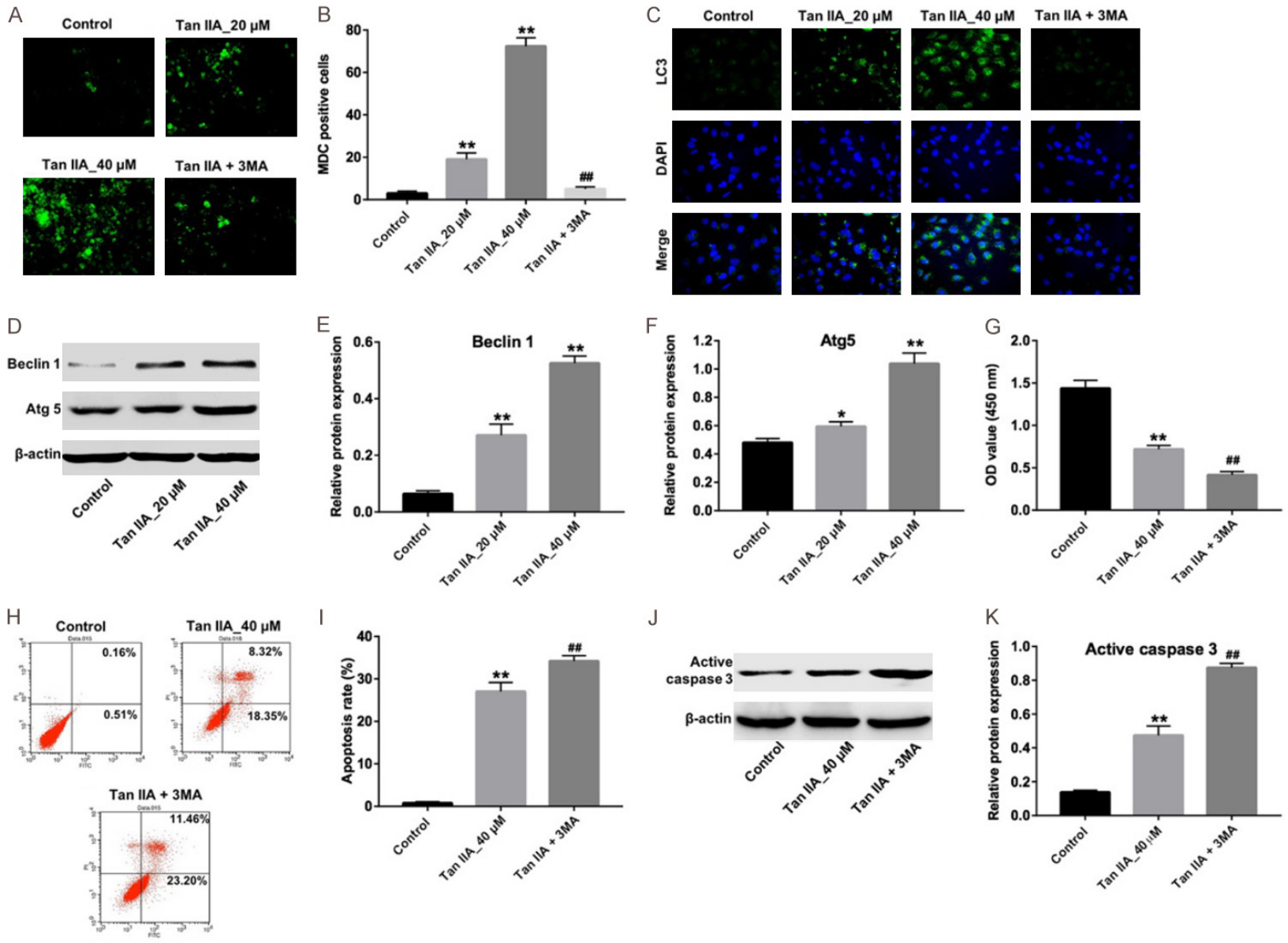
A
Control
Tan IIA_20 μM
Tan IIA_40 μM
Tan IIA + 3MA
B
MDC positive cells
Control
Tan IIA_20 μM
Tan IIA_40 μM
Tan IIA + 3MA
C
Control
Tan IIA_20 μM
Tan IIA_40 μM
Tan IIA + 3MA
LC3
DAPI
Merge
D
Beclin 1
Atg 5
β-actin
Control
Tan IIA_20 μM
Tan IIA_40 μM
E
Beclin 1
Relative protein expression
F
Atg5
Relative protein expression
G
OD value (450 nm)
H
Control
Tan IIA_40 μM
Tan IIA + 3MA
0.16%
0.51%
8.32%
18.35%
11.46%
23.20%
I
Apoptosis rate (%)
J
Active caspase 3
β-actin
K
Active caspase 3
Relative protein expression

Figure 4. Inhibition of autophagy enhanced Tan IIA-induced apoptosis in U937 cells. A. U937 cells were incubated with 5 mM 3MA for 1 h. Then, the culture medium was changed and cells were incubated with 40 μM Tan IIA for another 72 h. MDC staining was used to observe the autophagosomes formatting, × 200 magnification. B. The number of autophagosomes in cells were counted. C. Relative fluorescence expressions were quantified by LC3 and DAPI staining, × 400 magnification. D. U937 cells were exposed to 20 or 40 μM Tan IIA for 72 h. The expressions of beclin 1 and Atg5 in cells were analyzed by western blotting. E. The expression of Beclin 1 was quantified by normalizing to β-actin. F. The expression of Atg5 was quantified by normalizing to β-actin. G. U937 cells were incubated with 5 mM 3MA for 1 h. Then, the culture medium was changed and cells were incubated with 40 μM Tan IIA for another 72 h. Cell viability was determined using CCK-8 assay. H. Apoptotic cells were detected with Annexin V and PI double staining. I. The apoptosis cell rates were calculated. J. The expression of active caspase 3 in cells was analyzed by western blotting. K. Active caspase 3 relative expression was quantified by normalizing to β-actin. *P < 0.05, **P < 0.01 vs. control; ##P < 0.01 vs. Tan IIA group.

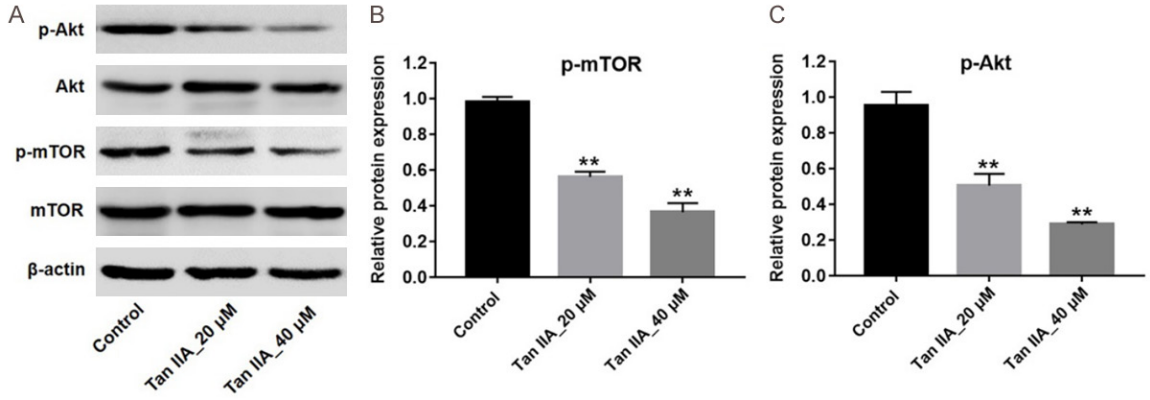

Figure 5. Tan IIA induced autophagy in U937 cells via inhibition of the Akt/mTOR pathway. U937 cells were exposed to 20 or 40 μM Tan IIA for 72 h. A. Expressions of p-Akt and p-mTOR in U937 cells were analyzed by western blotting. B. The expression of p-Akt was quantified by normalizing to Akt. C. The expression of p-mTOR was quantified by normalizing to mTOR. **P < 0.01 vs. control.

cal cancer xenograft in vivo. Lin et al studied that Tan IIA markedly inhibited the growth of breast cancer cells *in vitro* and *in vivo* [24]. Sui et al found that Tan IIA suppressed the growth of human colorectal cancer *in vitro* and *in vivo* [25]. All these findings suggest that Tan IIA exhibits notable anti-tumor effects on different tumor types.

Most malignant tumors exhibit a highly migratory and invasive effects [26]. Portulacerebroside A inhibited migration and invasion abilities of leukemia HL60 and U937 cells [19]. Zhang et al found that Tan IIA inhibited proliferation, migration and invasion in osteosarcoma MG-63 cells [10]. In the present study, our results revealed that Tan IIA could inhibit migration and invasion of U937 cells *in vitro*. Our findings were consistent with these results.

In the present study, our results indicated that Tan IIA significantly upregulated the levels of active caspase 3 and Bax, while downregulated the level of Bcl-2 *in vitro*. Zhang et al found that Tan IIA could induce cell apoptosis in human gastric cancer cells via upregulating the level of caspase 3 and downregulating the level of Bcl-2 [27]. These data revealed that Tan IIA could induce U937 cells apoptosis.

Previous report studied that PI3K/Akt/mTOR pathway performed an important role in the pathogenesis progression of leukemia [28]. In addition, PI3K/Akt/mTOR signaling pathway could regulate apoptosis and autophagy in U937 cells [28]. The novel finding in this study is that Tan IIA could downregulate the expressions of p-Akt and p-mTOR *in vitro* and *in vivo*. Similarly, su revealed that Tan IIA also could inhibit apoptosis in pancreatic cancer cells via inhibiting PI3K/AKT/mTOR pathways [29]. Su et al revealed that Tan IIA inhibited tumor growth in gastric carcinoma via downregulating the PI3K/Akt/mTOR *in vitro* and *in vivo* [30]. These results indicated that Tan IIA induced U937 cells apoptosis via inhibiting AKT/mTOR pathway.

In this study we also found Tan IIA could induce autophagy in U937 cells via increasing the lev-

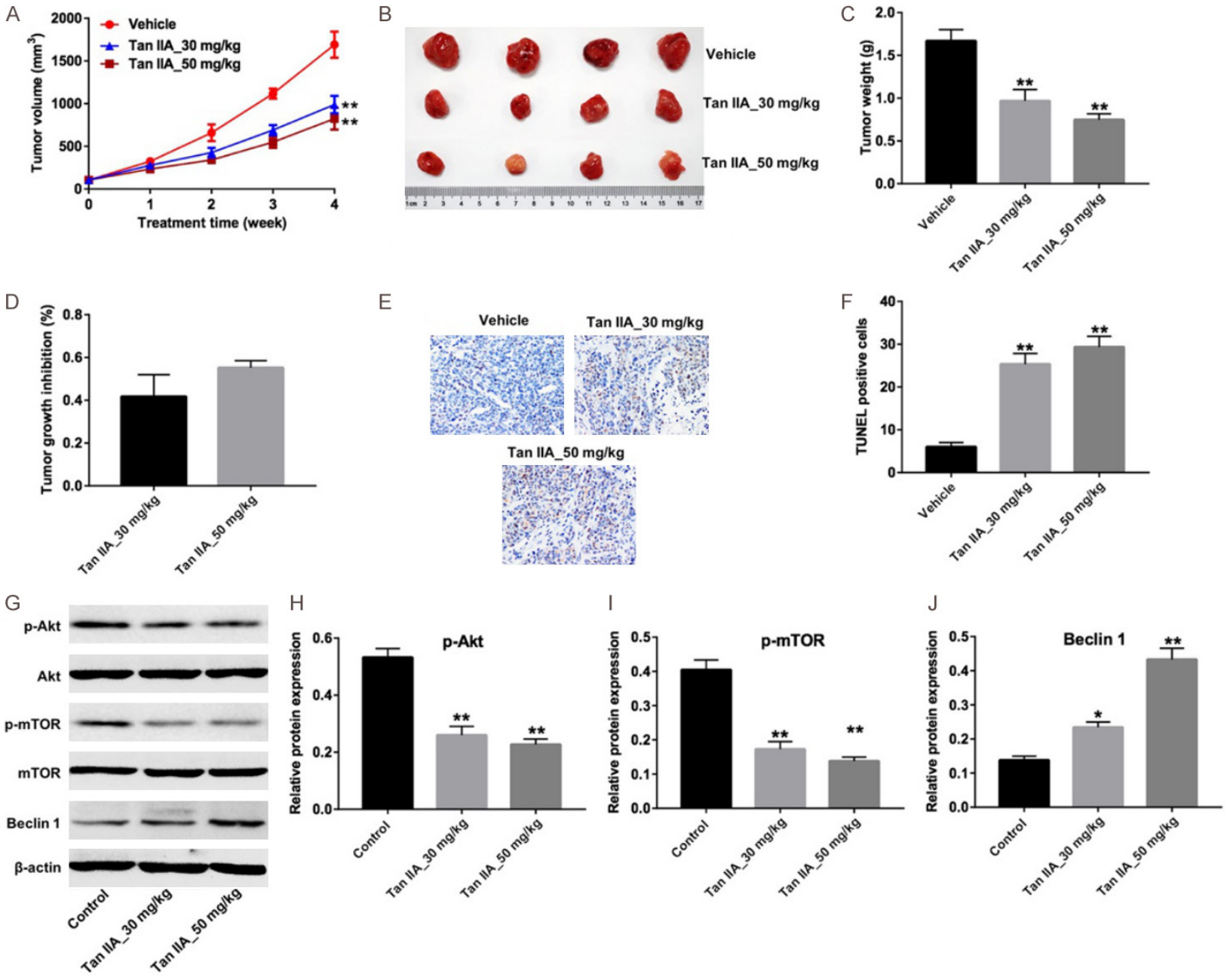
A
Vehicle
Tan IIA_30 mg/kg
Tan IIA_50 mg/kg
Tumor volume (mm3)
Treatment time (week)
B
Vehicle
Tan IIA_30 mg/kg
Tan IIA_50 mg/kg
C
Tumor weight (g)
D
Tumor growth inhibition (%)
E
Vehicle
Tan IIA_30 mg/kg
Tan IIA_50 mg/kg
F
TUNEL positive cells
G
p-Akt
Akt
p-mTOR
mTOR
Beclin 1
β-actin
Control
H
p-Akt
Relative protein expression
I
p-mTOR
J
Beclin 1

Figure 6. Tan IIA inhibited tumor growth via induction of apoptosis *in vivo*. A. Tumor volume of nude mice treated with Tan IIA (0, 30 or 50 mg/kg) for 4 weeks. The tumor volumes were monitored weekly. B. Tumors were isolated and pictured after 4 weeks' treatment. C. Tumor weights of mice were calculated. D. The inhibition rates of tumor growth were calculated. E, F. TUNEL staining of tumor tissues in each group and TUNEL positive cell rate were calculated. G. Expressions of p-Akt, p-mTOR and Beclin 1 in tumor tissues were analyzed by western blotting. H. Relative expression of p-Akt was quantified by normalizing to Akt. I. Relative expression of p-mTOR was quantified by normalizing to mTOR. J. Relative expression of Beclin 1 was quantified by normalizing to β-actin. **P < 0.01 vs. vehicle group.

els of Beclin 1 and Atg 5. Tan IIA could induce cell autophagy in oral squamous cell carcinoma cells via activation of Beclin-1/Atg 5 signaling and inhibition of PI3K/Akt/mTOR signaling [12]. Ding et al found that Tan IIA induced autophagy and apoptosis in glioma cells via inhibiting PI3K/Akt/mTOR signaling pathway and increasing the expression of LC3 and Beclin 1 [8]. Similar to these results, Tan IIA induced U937 cell apoptosis and autophagy via inhibiting PI3K/Akt/mTOR pathway *in vitro* and *in vivo*.

Recent study has shown that autophagy promoted AML cells survival [31]. Li et al revealed that Tan IIA induced apoptosis and autophagy, and inhibition of autophagy could increase Tan IIA-induced apoptosis in human prostate cancer PC-3 cells [32]. In the current study, we also found that inhibition of autophagy enhanced the Tan IIA-induced apoptosis in U937 cells. These findings suggested that autophagy may play a pro-survival role in U927 cells.

Conclusion

In this study, these results indicated that Tan IIA could induce apoptosis and autophagy in U937 cells via inhibiting PI3K/Akt/mTOR signaling pathway. In addition, inhibition of autophagy could enhance Tan IIA-induced apoptosis in U937 cells. In conclusion, we suggested that Tan IIA could be a potent agent for the treatment of patients with AML.

Disclosure of conflict of interest

None.

Address correspondence to: Dr. Aili He, Department of Hematology, The Second Affiliated Hospital of Xi'an Jiaotong University, No. 157 West Five Road, New Urban District, Xi'an 710004, Shanxi, P. R. China. E-mail: ailihe88@126.com

References

[1] Wang Y, Ma L, Wang C, Sheng G, Feng L, Yin C. Autocrine motility factor receptor promotes the proliferation of human acute monocytic leukemia THP-1 cells. Int J Mol Med 2015; 36: 627-632.

[2] Villeneuve P, Kim DT, Xu W, Brandwein J, Chang H. The morphological subcategories of acute monocytic leukemia (M5a and M5b) share similar immunophenotypic and cytogenetic features and clinical outcomes. Leuk Res 2008; 32: 269-273.

[3] Guo H, Lin SY, Ren WX, Lei Q, Chen ZC, Zhang L, Li QB. Enhanced response of acute monocytic leukemia cells to low-dose cytarabine by 1,25-dihydroxyvitamin D3. Curr Med Sci 2018; 38: 35-42.

[4] Dohner H, Weisdorf DJ, Bloomfield CD. Acute myeloid leukemia. N Engl J Med 2015; 373: 1136-1152.

[5] Ravindranath Y, Chang M, Steuber CP, Becton D, Dahl G, Civin C, Camitta B, Carroll A, Raimondi SC, Weinstein HJ; Pediatric Oncology Group. Pediatric Oncology Group (POG) studies of acute myeloid leukemia (AML): a review of four consecutive childhood AML trials conducted between 1981 and 2000. Leukemia 2005; 19: 2101-2116.

[6] Smith FO, Alonzo TA, Gerbing RB, Woods WG, Arceci RJ; Children's Cancer G. Long-term results of children with acute myeloid leukemia: a report of three consecutive Phase III trials by the Children's Cancer Group: CCG 251, CCG 213 and CCG 2891. Leukemia 2005; 19: 2054-2062.

[7] Johnston DL, Alonzo TA, Gerbing RB, Lange BJ, Woods WG. Risk factors and therapy for isolated central nervous system relapse of pediatric acute myeloid leukemia. J Clin Oncol 2005; 23: 9172-9178.

[8] Ding L, Ding L, Wang S, Wang S, Wang W, Wang W, Lv P, Lv P, Zhao D, Zhao D, Chen F, Chen F, Meng T, Meng T, Dong L, Dong L, Qi L, Qi L. Tanshinone IIA affects autophagy and apoptosis of glioma cells by inhibiting phosphatidylinositol 3-Kinase/Akt/Mammalian target of rapamycin signaling pathway. Pharmacology 2017; 99: 188-195.

[9] Wang Z, Yang X, Zhang W, Zhang P, Jiang B. Tanshinone IIA attenuates nerve structural and functional damage induced by nerve crush injury in rats. PLoS One 2018; 13: e0202532.

[10] Zhang Y, Wei RX, Zhu XB, Cai L, Jin W, Hu H. Tanshinone IIA induces apoptosis and inhibits

the proliferation, migration, and invasion of the osteosarcoma MG-63 cell line in vitro. Anticancer Drugs 2012; 23: 212-219.
[11] Ren B, Zhang YX, Zhou HX, Sun FW, Zhang ZF, Wei Z, Zhang CY, Si DW. Tanshinone IIA prevents the loss of nigrostriatal dopaminergic neurons by inhibiting NADPH oxidase and iNOS in the MPTP model of Parkinson's disease. J Neurol Sci 2015; 348: 142-152.
[12] Qiu Y, Li C, Wang Q, Zeng X, Ji P. Tanshinone IIA induces cell death via Beclin-1-dependent autophagy in oral squamous cell carcinoma SCC-9 cell line. Cancer Med 2018; 7: 397-407.
[13] Yin X, Yin Y, Cao FL, Chen YF, Peng Y, Hou WG, Sun SK, Luo ZJ. Tanshinone IIA attenuates the inflammatory response and apoptosis after traumatic injury of the spinal cord in adult rats. PLoS One 2012; 7: e38381.
[14] Chen Y, Wu X, Yu S, Lin X, Wu J, Li L, Zhao J, Zhao Y. Neuroprotection of tanshinone IIA against cerebral ischemia/reperfusion injury through inhibition of macrophage migration inhibitory factor in rats. PLoS One 2012; 7: e40165.
[15] Zhang L, Tong X, Li J, Huang Y, Hu X, Chen Y, Huang J, Wang J, Liu B. Apoptotic and autophagic pathways with relevant small-molecule compounds, in cancer stem cells. Cell Prolif 2015; 48: 385-397.
[16] Metgud R, Gupta K. Expression of cell cycle and apoptosis-related proteins in ameloblastoma and keratocystic odontogenic tumor. Ann Diagn Pathol 2013; 17: 518-521.
[17] Shao B, Li CW, Lim SO, Sun L, Lai YJ, Hou J, Liu C, Chang CW, Qiu Y, Hsu JM, Chan LC, Zha Z, Li H, Hung MC. Deglycosylation of PD-L1 by 2-deoxyglucose reverses PARP inhibitor-induced immunosuppression in triple-negative breast cancer. Am J Cancer Res 2018; 8: 1837-1846.
[18] Li Q, Shen L, Wang Z, Jiang HP, Liu LX. Tanshinone IIA protects against myocardial ischemia reperfusion injury by activating the PI3K/Akt/mTOR signaling pathway. Biomed Pharmacother 2016; 84: 106-114.
[19] Ye Q, Liao X, Fu P, Dou J, Chen K, Jiang H. Portulacerebroside A inhibits adhesion, migration, and invasion of human leukemia HL60 cells and U937 cells through the regulation of p38/JNK signaling pathway. Onco Targets Ther 2016; 9: 6953-6963.
[20] Vurusaner B, Gargiulo S, Testa G, Gamba P, Leonarduzzi G, Poli G, Basaga H. The role of autophagy in survival response induced by 27-hydroxycholesterol in human promonocytic cells. Redox Biol 2018; 17: 400-410.
[21] Wang RC, Wei Y, An Z, Zou Z, Xiao G, Bhagat G, White M, Reichelt J, Levine B. Akt-mediated regulation of autophagy and tumorigenesis through Beclin 1 phosphorylation. Science 2012; 338: 956-959.
[22] Lin LL, Hsia CR, Hsu CL, Huang HC, Juan HF. Integrating transcriptomics and proteomics to show that tanshinone IIA suppresses cell growth by blocking glucose metabolism in gastric cancer cells. BMC Genomics 2015; 16: 41.
[23] Lin LL, Hsia CR, Hsu CL, Huang HC, Juan HF. Integrating transcriptomics and proteomics to show that tanshinone IIA suppresses cell growth by blocking glucose metabolism in gastric cancer cells. BMC Genomics 2015; 16: 41.
[24] Lin C, Wang L, Wang H, Yang L, Guo H, Wang X. Tanshinone IIA inhibits breast cancer stem cells growth in vitro and in vivo through attenuation of IL-6/STAT3/NF-kB signaling pathways. J Cell Biochem 2013; 114: 2061-2070.
[25] Sui H, Zhao J, Zhou L, Wen H, Deng W, Li C, Ji Q, Liu X, Feng Y, Chai N, Zhang Q, Cai J, Li Q. Tanshinone IIA inhibits beta-catenin/VEGF-mediated angiogenesis by targeting TGF-beta1 in normoxic and HIF-1alpha in hypoxic microenvironments in human colorectal cancer. Cancer Lett 2017; 403: 86-97.
[26] Ma X, Miao H, Jing B, Pan Q, Zhang H, Chen Y, Zhang D, Liang Z, Wen Z, Li M. Claudin-4 controls the proliferation, apoptosis, migration and in vivo growth of MCF-7 breast cancer cells. Oncol Rep 2015; 34: 681-690.
[27] Zhang Y, Guo S, Fang J, Peng B, Zhang Y, Cao T. Tanshinone IIA inhibits cell proliferation and tumor growth by downregulating STAT3 in human gastric cancer. Exp Ther Med 2018; 16: 2931-2937.
[28] Kumar D, Das B, Sen R, Kundu P, Manna A, Sarkar A, Chowdhury C, Chatterjee M, Das P. Andrographolide analogue induces apoptosis and autophagy mediated cell death in U937 cells by Inhibition of PI3K/Akt/mTOR pathway. PLoS One 2015; 10: e0139657.
[29] Chiu TL, Su CC. Tanshinone IIA increases protein expression levels of PERK, ATF6, IRE1-alpha, CHOP, caspase3 and caspase12 in pancreatic cancer BxPC3 cellderived xenograft tumors. Mol Med Rep 2017; 15: 3259-3263.
[30] Su CC, Chiu TL. Tanshinone IIA decreases the protein expression of EGFR, and IGFR blocking the PI3K/Akt/mTOR pathway in gastric carcinoma AGS cells both in vitro and in vivo. Oncol Rep 2016; 36: 1173-1179.
[31] Chao TL, Wang TY, Lee CH, Yiin SJ, Ho CT, Wu SH, You HL, Chern CL. Anti-Cancerous effect of inonotus taiwanensis polysaccharide extract on human acute monocytic leukemia cells through ROS-independent intrinsic mitochondrial pathway. Int J Mol Sci 2018; 19.
[32] Li C, Han X, Zhang H, Wu J, Li B. The interplay between autophagy and apoptosis induced by tanshinone IIA in prostate cancer cells. Tumour Biol 2016; 37: 7667-7674.